

Non-destructive characterization of zirconia-toughened alumina ceramics using ultrasonics

D. BASU, S. MUKHERJEE, K. K. PHANI

Central Glass and Ceramic Research Institute, Jadavpur University, Calcutta 700032, India

Ultrasonics has been used for the characterization of sintered zirconia-toughened alumina (ZTA) ceramics. The variation of ultrasonic velocity with volume fraction of zirconia in an alumina matrix was studied. Variation of ultrasonic velocity with volume fraction of ZrO_2 content was analysed in terms of a second-degree polynomial in the volume fraction of ZrO_2 . The elastic moduli and Poisson's ratio evaluated from the longitudinal and shear velocities have also been described in terms of a similar equation. The observed variation in velocity and moduli with porosity has been compared with the predicted values based on elasticity theory.

1. Introduction

In the last few decades, considerable interest has been developed in the non-destructive ultrasonic characterization of ceramics, electrical porcelain and other porous materials, for their physical and elastic properties [1–5]. Clay based ceramics have also been investigated to find the effect of compaction parameters on the sintered properties [6] and establish the correlation between the physical properties and pore volume fraction [7]. In recent years studies have been carried out on ultrasonic characterization of multi-phase composites such as graphite/epoxy composites [8–12], aluminium/aramid-epoxy composite [13], multidirectional composite laminate [14], etc. Lu *et al.* [15] evaluated silicon carbide-reinforced aluminium metal matrix composites and tried to establish the effect of porosity on the ultimate physical and elastic properties, while Jagnoux *et al.* [16] studied the interface in single SiC fibre-reinforced aluminium composites using a similar technique. However, it seems that ultrasonic characterization of particulate-toughened ceramics, to the best of our authors' knowledge, has not received much attention. An attempt has therefore been made in this work to characterize zirconia-toughened alumina, to evaluate the elastic constants, and find the correlation between physical properties and volume fraction of zirconia content.

2. Experimental procedure

2.1. Specimens

Powders of alumina (XA-16, USA) and varying amounts of zirconia, partially stabilized with 3 mol % Y_2O_3 (3Y-TZP, Tayosoda Corporation, Japan) were milled in a planetary ball mill in isopropanol medium to prepare the basic composite powders. The particle size and the chemical analysis of the powders are given

in Table I. The mixture was subsequently dried and calcined at 700 °C. The calcined product was reground in isopropanol and polyvinyl alcohol was added during grinding. These powders were uniaxially pressed into plates of $25 \times 25 \times 5$ mm³ dimensions at 120 MPa. The green compacts were sintered at 1550 °C for 2 h in air. The sintered samples were subsequently surface ground and polished with a lap-master to maintain the surface parallelity of the faces within 1 µm.

The bulk density, ρ , of the sintered body of various ZTA compositions was measured by the water displacement method while their theoretical density, ρ_0 , was calculated from the available atomic weights and unit cell dimensions. The total porosity was then calculated from the relation

$$P = 1 - \rho/\rho_0 \quad (1)$$

where P is the pore volume fraction.

2.2. Ultrasonic velocity measurement

The ultrasonic velocity (transverse and longitudinal) was measured using the ultrasonic Tester USIP 12 (Kraut Kramer) interfaced with a 100 MHz oscilloscope (Philips model 3350). The centre frequency of the transducer (10 mm diameter) was 15 and 5 MHz for longitudinal and transverse waves, respectively. The pulse-echo method was used for calculating the velocity. The transient time could be measured within an accuracy of ± 5 ns.

3. Results

3.1. Ultrasonic velocity

Table II gives the ultrasonic velocity of samples of different ZrO_2 content together with the estimated

TABLE I Chemical analysis of alumina and 3Y-PSZ powders

Constituents (wt %)	Alumina (grade XA-16 supplied by Alcoa)	3Y-PSZ (supplied by Tayosoda)
Y ₂ O ₃	—	5.07
Al ₂ O ₃	Balance	< 0.005
ZrO ₂	Trace	Balance
SiO ₂	0.02	< 0.002
Fe ₂ O ₃	0.006	< 0.002
Na ₂ O	0.07	0.015
Loss on ignition	—	0.71

porosity values. It may be seen from the table that the porosity of the sample is less than 8%, though they differ from sample to sample.

In a recent review of the data available on porous polycrystalline materials, Roth *et al.* [17] showed that the ultrasonic velocity, V , variation with porosity, P , is given by the relation

$$V = V_0 (1 - P) \quad (2)$$

where V_0 is the velocity for zero porosity. Thus, for comparison of ultrasonic velocity variation with volume fraction of ZrO₂ zero porosity values are obtained from the above relation using the measured velocity and porosity data. Those values are also given in Table II. Fig. 1 presents the plot of longitudinal, V_l , and transverse, V_s , ultrasonic velocity against volume fraction of zirconia.

The measured values were fitted to an equation of the form

$$V_l = V_{l0} (1 - a\phi + b\phi^2) \quad (3)$$

$$V_s = V_{s0} (1 - a_1\phi + b_1\phi^2) \quad (4)$$

where V_{l0} and V_{s0} are the ultrasonic velocities in pure alumina, a , b , a_1 , b_1 are constants and ϕ is the volume fraction of zirconia.

The above relations were derived from Hashin's relation from elastic moduli of a two-phase material [18]. For a two-phase material, Hashin gave a good

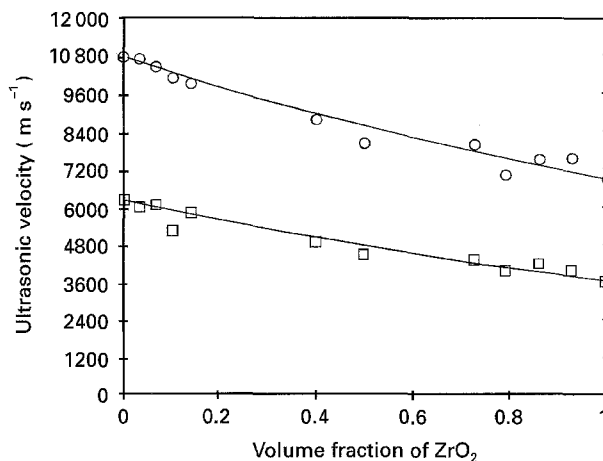


Figure 1 Variation of (○) longitudinal and (□) transverse velocity with volume fraction of ZrO₂ in sintered ZTA ceramics. (—) Fitted Equations 10 and 11.

approximation of the shear modulus

$$G^*/G_m = 1 + \frac{A(D-1)\phi}{1 + C[D - (D-1)\phi]} \quad (5)$$

where G^* is the shear modulus of the two-phase system, G_m is the shear modulus of the matrix, A , C , D are constant for a particular combination of the matrix and inclusion, A and C are functions of Poisson's ratio of the matrix, and D is the ratio of shear modulus of inclusion and the matrix.

Equation 5 can be further simplified to the form

$$G^*/G_m = \frac{1 - C_1\phi}{1 - B_1\phi} \quad (6)$$

where C_1 and B_1 are again functions of the constants A , C and D , because

$$V_s^2 = G^*/\rho^* = \frac{G^*}{\rho_m(1 - \phi) + \rho_1\phi} \quad (7)$$

where ρ_1 and ρ_m are the densities of the inclusion and the matrix, respectively.

TABLE II Ultrasonic velocities of ZTA ceramics

ZrO ₂ (vol %)	Density (g cm ⁻³)	Porosity (%)	Measured long. vel. (m s ⁻¹)	Measured trans. vel (m s ⁻¹)	Longitudinal vel. for zero porosity (m s ⁻¹)	Transverse vel. for zero porosity (m s ⁻¹)
0	3.95	1.00	10724.1	6242.4	10832.4	6305.5
3.3	4.04	1.20	10609.9	6000.0	10740.9	6074.1
6.8	4.13	1.20	10374.7	6052.6	10500.7	6126.1
10.4	4.22	0.90	10053.1	5241.4	10148.5	5291.1
14.1	4.28	1.40	9821.1	5789.5	9958.5	5870.5
39.6	4.68	7.20	8158.4	4564.3	8791.4	4918.4
49.6	4.90	7.90	7403.6	4138.2	8038.7	4493.2
72.4	5.48	2.50	7638.3	4133.0	7834.2	4238.9
78.8	5.54	2.00	7017.2	3970.7	7160.5	4051.7
85.5	5.62	3.60	7219.0	4043.0	7488.6	4194.0
92.6	5.71	4.00	7238.0	3814.8	7539.6	3973.4
100	6.02	1.00	6815.5	3591.8	6883.7	3627.8

Combining Equations 6 and 7

$$V_s^2 = V_{s0}^2 \frac{(1 - C_1\phi)}{(1 - B_1\phi)(1 - f_1\phi)} \quad (8)$$

where f_1 is the density ratio between inclusion and matrix. Expanding the terms of Equation 7 binomially, and neglecting terms higher than second order in ϕ , yields Equation 4. For longitudinal velocity, a similar relationship was also assumed.

Equations 3 and 4 were fitted to the data by regression analysis. The sum of squares, Q , was used as the measure of the goodness of the fit between the fitted equation and the data

$$Q = 1 - \frac{\sum_{i=1}^n (M_i - \hat{M}_i)^2}{\sum_{i=1}^n (M_i - \bar{M}_i)^2} \quad (9)$$

where \hat{M}_i is the value calculated from the fitted equation for an appropriate ϕ value. M_i and \bar{M}_i are the measured values and mean value, respectively. For a good fit $Q > 0.95$; for $Q < 0.9$, the fit is poor. The equations that fit the data are:

longitudinal velocity

$$V_l (\text{m s}^{-1}) = 10871.94 (1 - 0.61\phi + 0.268\phi^2) \quad (10)$$

shear velocity

$$V_s (\text{m s}^{-1}) = 6191.88 (1 - 0.626\phi + 0.243\phi^2) \quad (11)$$

with Q values of 0.98 and 0.95, respectively, for longitudinal and shear ultrasonic velocities, indicating a good agreement between the fitted equation and the data, the extrapolated values for ultrasonic longitudinal and shear velocities for pure alumina (i.e. $\phi = 0$) and pure zirconia (i.e. $\phi = 1$) work out to be 10871.9, 6191.9 and 7153.7, 3820.4 m s^{-1} , respectively. These values compare favourably with the respective values of theoretically dense alumina for longitudinal and shear velocities of 10845 and 6373 m s^{-1} , and 9920 and 6350 m s^{-1} , obtained by Spriggs [19] and Natarajan [20], respectively. In the absence of any reported values of theoretically dense zirconia ceramics with 3 mol% Y_2O_3 , other extrapolated values obtained in this work for $\phi = 1$ could not be compared. However, Kandil *et al.* [22] reported the longitudinal and transverse ultrasonic velocities of ZrO_2 with 8 mol% Y_2O_3 as 7100 and 3060 m s^{-1} , respectively. These values are in fair agreement with the present values of ZrO_2 with 3 mol% Y_2O_3 .

Theoretically, the ultrasonic velocities of two-phase materials can be estimated from the relation

$$V_l = \left[\frac{K + 4/3G}{\rho} \right]^{1/2} \quad (12)$$

$$V_s = \left[\frac{G}{\rho} \right]^{1/2} \quad (13)$$

where K and G are the theoretically estimated bulk modulus and shear modulus of two-phase systems. The theoretical estimate of K and G can be obtained

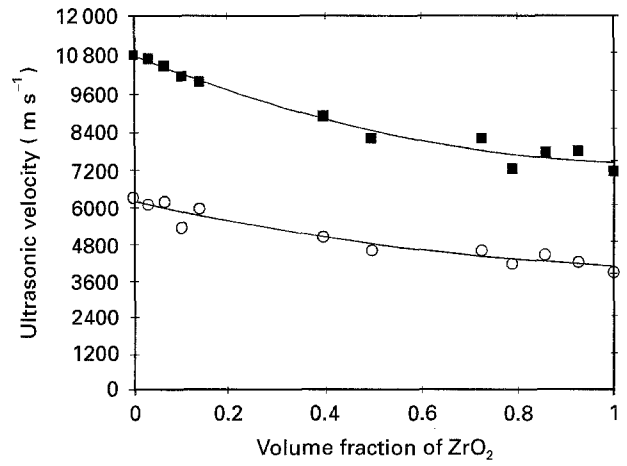


Figure 2 Comparison of ultrasonic velocity variation in sintered ZTA ceramics with (—) the theoretically predicted values: (■) longitudinal, (○) transverse.

from the Hashin's elasticity theory which considers the change in strain energy in a loaded homogeneous body due to the presence of non-homogeneity. The theoretical values of the module were estimated using from the bounds of bulk modulus and the approximate expression for shear modulus. Equations 12 and 13 were then used for calculating theoretical velocity values. These estimated values, along with the experimental data, are presented in Fig. 2. The predicted values are in close agreement with the experimental data. In deriving these values, the bulk shear moduli of theoretically dense alumina were taken as 251.0 and 162.9 GPa, respectively. These values were estimated by Anderson *et al.* [21] from measured single-crystal elastic constants.

It may be noted here that the theory assumes a spherical shape of the inclusion. Thus the close agreement between theory and experiment indicates that zirconia grains are nearly spherical in shape. This is confirmed from the micrographs shown in Fig. 3 for volume fraction of zirconia samples.

3.2. Elastic moduli

The elastic moduli of the samples were calculated from the measured ultrasonic velocities using the equations: Young's modulus

$$E = \frac{\rho V_s^2 (3V_l^2 - 4V_s^2)}{(V_l^2 - V_s^2)} \quad (14)$$

shear modulus

$$G = \rho V_s^2 \quad (15)$$

Poisson's ratio

$$\nu = \frac{(V_l^2/2 - V_s^2)}{(V_l^2 - V_s^2)} \quad (16)$$

Fig. 4 presents the Young's and shear moduli plotted against the volume fraction of ZrO_2 . Again, equations

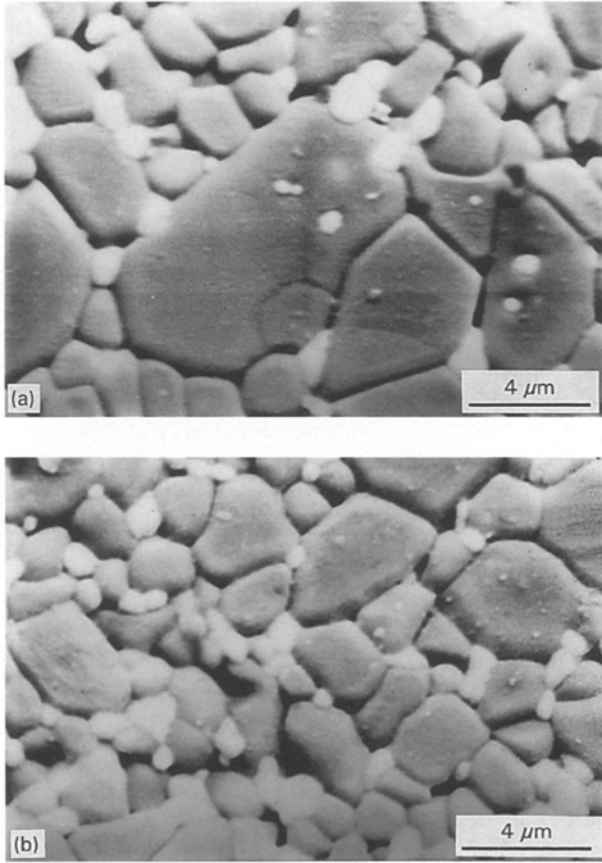


Figure 3 Micrographs of ZTA ceramics (a) with 3.3% and (b) 10.4% ZrO_2 showing the nearly spherical shape of ZrO_2 grains.

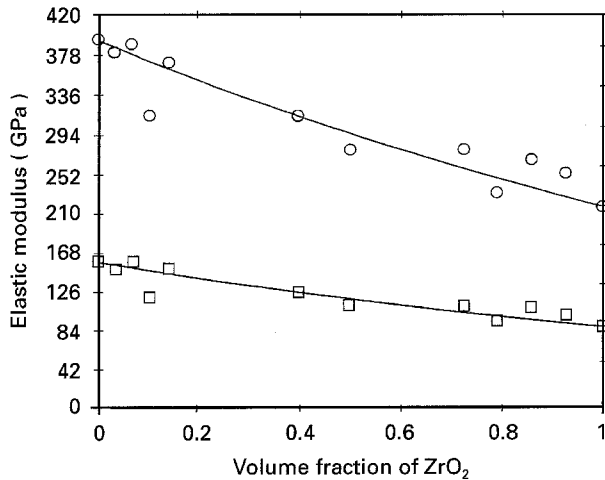


Figure 4 Variation of elastic moduli of sintered ZTA ceramics with volume fraction of ZrO_2 . (—) Fitted Equations 19 and 20, respectively: (○) Young's, (□) shear moduli.

of the form

$$E = E_m (1 - a\phi + b\phi^2) \quad (17)$$

and

$$G = G_m (1 - a_1\phi + b_1\phi^2) \quad (18)$$

were fitted to the experimental data by regression analysis. This yielded the relations

$$E \text{ (GPa)} = 386.3 (1 - 0.63\phi + 0.21\phi^2) \quad (19)$$

$$G \text{ (GPa)} = 153.9 (1 - 0.65\phi + 0.21\phi^2) \quad (20)$$

TABLE III Comparison of elastic moduli values reported in the literature

Material	Young's modulus (GPa)		Shear modulus (GPa)	
Alumina	386.3	Present work	153.9	Present work
	402.0	[23]	160.6	[21]
	397.0	[24]	163.3	[22]
Zirconia	227.1	Present work	87.6	Present work
	209.0	[25]	—	
	207.0	[26]	—	

giving Q values of 0.898 and 0.875, respectively. These equations are again plotted in Fig. 4 showing good agreement with the data.

The extrapolated value of Young's and shear moduli of pure alumina and zirconia are obtained as 386.3 and 153.9, and 227.14 and 87.6 GPa, respectively. These values, along with those reported in the literature, are compared in Table III.

Table III shows that the extrapolated values are in fairly good agreement with the values reported in the literature. The theoretical values of elastic moduli were also calculated using Hashin's theory. The calculated, as well as the measured, values are plotted in Fig. 5. The variation in moduli predicted by the theory agrees fairly well with the observed values. This again confirms the spherical nature of the ZrO_2 grains. A more sensitive test of the power of theory is a comparison between the bulk modulus and Poisson's ratio and values of these isotropic elastic constants calculated from the values of E and G . This comparison is shown in Fig. 6. The closeness of these calculated values with the theoretical curve is remarkable considering the sensitivity of this calculation to the propagation of experimental errors. Particularly for Poisson's ratio, this sensitivity is magnified around low-volume fractions of zirconia due to the subtraction of two almost equal terms.

4. Discussion

It has been observed that variation of ultrasonic velocity in zirconia-toughened alumina can be described by a second-degree polynomial in the volume fraction of zirconia, given by Equation 3. The observed variations are also in close agreement with the theory based on spherical particle inclusion. The dependence on elastic moduli of the volume fraction of inclusions, also follows a similar equation. Thus a good correlation can be expected between the velocity and modulus. A plot of elastic modulus against ultrasonic velocity (Fig. 7) confirms this. Similar observations in other ceramics like uranium dioxide-sintered iron compacts and silicon carbide [2, 5], have already been reported in the literature. The data points are fitted into a straight line

$$E = -86.04 + 0.046 V_1 \quad (21)$$

with a Q value of 0.92. Thus longitudinal velocity alone can be used for monitoring Young's modulus of

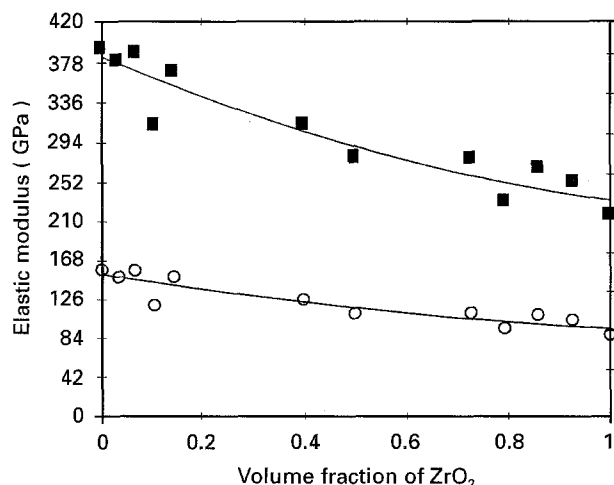


Figure 5 Comparison of elastic moduli of sintered ZTA ceramics with the theoretically predicted values. (■) Young's, (○) shear moduli.

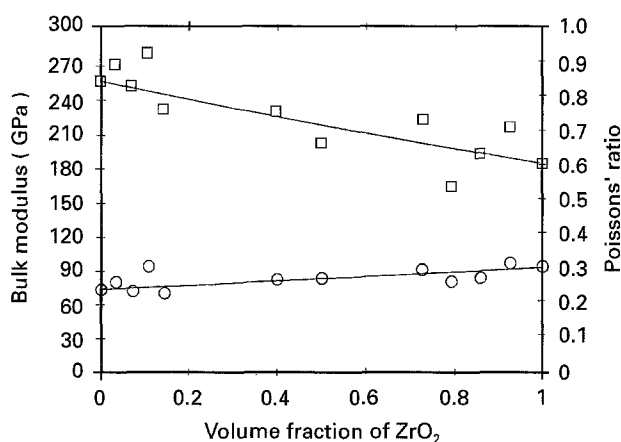


Figure 6 Variation of (□) bulk modulus and (○) Poisson's ratio of sintered ZTA ceramics with volume fraction of ZrO_2 . The theoretically predicted values.

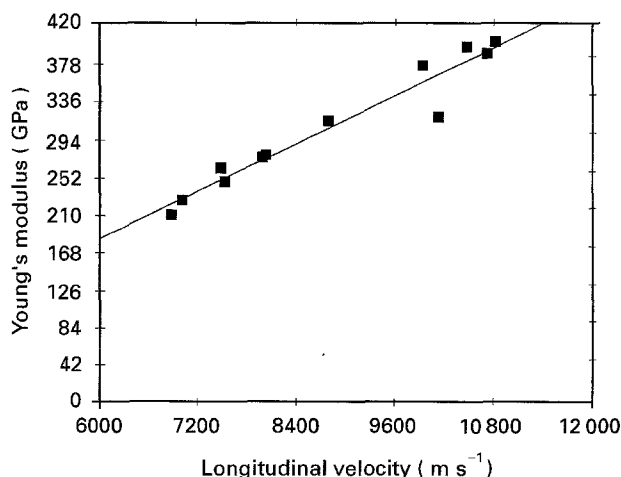


Figure 7 Plot of Young's modulus against longitudinal ultrasonic velocity in ZTA ceramics showing a linear fit.

this ceramic as a routine check in a production plant. It may also be noted that Equation 10 can also be used to estimate the volume fraction of zirconia present from the longitudinal velocity measurements.

5. Conclusions

Ultrasonic velocity of zirconia-toughened alumina ceramics in the volume fraction of zirconia range from 0%–100% were generated. The measured velocity values were fitted into second-degree polynomials which would serve as calibration graphs for using ultrasonic velocity for monitoring the volume fraction of zirconia in this type of ceramic. The values were compared with the existing theory of elasticity models based on spherical inclusions. The observed variation with volume fraction of inclusion agreed well with the theory. The micrographs also confirm the spherical nature of the inclusion phase.

The elastic moduli were evaluated from the ultrasonic velocity data and, here again, they agreed with the values predicted by the elasticity theory quite well. Analysis of the data further shows that there is good linear correlation between longitudinal ultrasonic velocity and Young's modulus over the entire volume fraction range. The results show that ultrasonic velocity may be used as a predictor of elastic moduli for this two-phase ceramic.

Acknowledgements

The authors thank Dr B. K. Sarkar, Director of the Institute, for his kind permission to publish this paper, Mr M. K. Basu, Head, Technical Ceramics Division of the Institute, for his interest in this work, and also Mr R. K. Ray, for typing the manuscript.

References

1. R. M. SPRIGGS, *J. Am. Ceram. Soc.* **44** (1961) 628.
2. S. HOWARD, J. TANI, H. ARNOLD, SCHWETLICK and W. SACHSE, in "NDE of microstructure for process control", Vol. II edited by H.N.G. Wadley (ASM, Ohio, 1985) p. 81.
3. A. NAGARAJAN, *J. Appl. Phys.* **42** (1971) 3693.
4. W. KREHER, J. RANACHOWSKI and F. RAJMUND, *Ultrasonics* **14** (1971) 70.
5. J. P. PANAKKAL, "Nondestructive evaluation of nuclear fuels by radiographic and ultrasonic technique". PhD thesis, Kerala University, India (1991).
6. B. TRISCH, W. R. THEILE and W. BERAWANGER, *Rep. Deut. Keram. Gesell. (DKG)* **63** (1986) 263.
7. J. P. PANAKKAL, *Br. J. Nondestr. Test.* **34** (1992) 529.
8. M. YAMATA and S. NOMAT-NASSER, *J. Compos. Mater.* **15** (1981) 531.
9. A. H. NAJFEH and D. E. CHIMENTI, *J. Appl. Mech.* **55** (1988) 863.
10. V. DONGAL and V. K. KINRA, *J. Acoust. Soc. Am.* **85** (1989) 2268.
11. A. K. MAL, *Wave Motion* **10** (1988) 257.
12. S. K. DATTA, A. H. SHAH, R. L. BRATTAN and T. CHAKRABORTY, *J. Acoust. Soc. Am.* **83** (1988) 2020.
13. P. J. SHULL and D. E. CHIMENTI, in "Review of Progress in Qualitative Nondestructive Evaluation", Vol. 118, edited by D. O. Thomson and D. E. Chimenti (Plenum, New York, London, 1992) 1421.
14. J. LEE, *ibid.*, p. 1459.
15. Y. LU, P. K. LIAW, R. E. SHANNON, It Jeong and D. K. Hsu, *ibid.*, p. 1467.
16. P. JAGNOUX, R. FOUGERES and A. VINCENT, *ibid.*, p. 1475.
17. J. ROTH, D. B. SANG, S. M. SWICKARD and DE GUIRE, NASA Technical Memorandum 102501, July 1990, p. 3.
18. Z. HASHIN, *J. Appl. Mech.* **29** (1962) 143.
19. R. M. SPRIGGS, *J. Am. Ceram. Soc.* **44** (1961) 628.

20. A. NAGARAJAN, *J. Appl. Phys.* **42** (1971) 3693.
21. O. L. ANDERSON, E. SCHREIBER, R. C. LIEBERMAN and N. SOGA, *Rev. Geophys* **6** (1968) 491.
22. H. M. KANDIL, J. D. GREINER and J. F. SMITH, *J. Am. Ceram Soc.* **67** (1984) 341.
23. J. B. WACHTMAN, W. E. TEFFT, D. G. LAM and R. P. STINCHFIELD, *J. Res. Nat. Bur. Stand.* **64A** (1960) 213.
24. R. M. SPRIGGS, *J. Am. Ceram. Soc.* **44** (1962) 628
25. Y. OKAMOTO, J. IEUJI, Y. YAMADA, K. HAYASHI and T. NISHIKAWA, in "Advances in Ceramics", Vol. **24B**, edited by S. Somiya, N. Yamamoto and H. Hanagida, (American Ceramic Society, Columbus, Ohio, 1988) p. 565.
26. H. GREINER, E. KEIM, W. KLEINLEIN and E. WEIß, in "Proceedings of the 2nd International Conference on Solid Oxide Fuel Cells", edited by F. Grosz, P. Zeger, S. C. Singhal and O. Yamamoto (Commission of the European Communities, Luxembourg, 1991) p. 705.

*Received 19 August 1994
and accepted 7 June 1995*